Machine intelligence identifies soluble TNFa as a therapeutic target for spinal cord injury

JR Huie[1]*, AR Ferguson[1,2]*, N Kyritsis[1] , J Z Pan[3], K-A Irvine[4], JL Nielson[5,6] , PG Schupp[7], MC Oldham[7] , JC Gensel[8], A Lin[1], MR Segal[9], RR Ratan[10], JC Bresnahan[1], MS Beattie[1].

[1]Brain and Spinal Injury Center (BASIC), Department of Neurological Surgery, University of California San Francisco; [2]San Francisco Veterans Affairs Medical Center; [3]Department of Anesthesiology, University of California San Francisco; [4]Department of Anesthesiology, Perioperative and Pain Medicine, VA Palo Alto Healthcare System and Stanford University; [5]Department of Psychiatry & Behavioral Sciences, University of Minnesota; [6]Institute for Health Informatics, University of Minnesota; [7]Brain Tumor Research Center, University of California, San Francisco; [8]SCoBIRC, University of Kentucky; [9]Center for Bioinformatics and Molecular Biostatistics, Department of Epidemiology and Biostatistics, University of California San Francisco; [10]Burke-Cornell Medical Research Institute, Department of Neurology and Neuroscience, Weill Medical College of Cornell University.

Correspondence should be addressed to Adam R. Ferguson adam.ferguson@ucsf.edu and Michael S. Beattie michael.beattie@ucsf.edu, Brain and Spinal Injury Center (BASIC), Department of Neurological Surgery, University of California San Francisco, San Francisco, CA.

*Equal contribution

Acknowledgements: We would like to thank (in alphabetical order) Tomoo Inoue, Yvette Nout Ellen Stuck, and Jason Talbott for useful comments on a prior version of this manuscript. This work was funded by NIH grants NS067092 (A.R.F.), NS069537 (A.R.F), NS038079 (J.C.B. and M.S.B.), AG032518 (M.S.B. and J.C.B.), NYSCoRE CO19772 (M.S.B. and J.C.B.), and NIH UCSF Anesthesia T32 training grant (NIGMS T32GM008440) to JZP.

SUMMARY

Traumatic spinal cord injury (SCI) produces a complex syndrome that is expressed across multiple endpoints ranging from molecular and cellular changes to functional behavioral deficits. Effective therapeutic strategies for CNS injury are therefore likely to manifest multi-factorial effects across a broad range of biological and functional outcome measures. Thus, multivariate analytic approaches are needed to capture the linkage between biological and neurobehavioral outcomes. Injury-induced neuroinflammation (NI) presents a particularly challenging therapeutic target, since NI is involved in both degeneration and repair[1,2]. Here, we used big-data integration and large-scale analytics to examine a large dataset of preclinical efficacy tests combining 5 different blinded, fully counter-balanced treatment trials for different acute anti-inflammatory treatments for cervical spinal cord injury in rats. Multi-dimensional discovery, using topological data analysis[3] (TDA) and principal components analysis (PCA) revealed that only one showed consistent multidimensional syndromic benefit: intrathecal application of recombinant soluble TNFα receptor 1 (sTNFR1), which showed an inverse-U dose response efficacy. Using the optimal acute dose, we showed that clinically-relevant 90 min delayed treatment profoundly affected multiple biological indices of NI in the first 48 hrs after injury, including reduction in pro-inflammatory cytokines and gene expression of a coherent complex of acute inflammatory mediators and receptors. Further, a 90 min delayed bolus dose of sTNFR1 reduced the expression of NI markers in the chronic perilesional spinal

cord, and consistently improved neurological function over 6 weeks post SCI. These results provide validation of a novel strategy for precision preclinical drug discovery that is likely to improve translation in the difficult landscape of CNS trauma, and confirm the importance of TNFα signaling as a therapeutic target.

Numerous therapeutic targets have been identified for SCI, including treatments aimed at blunting or modulating the post-injury cascade of neuroinflammation[1]. But aspects of neuroinflammation are known to also initiate repair[4-7]. This multi-faceted aspect of neuroinflammation may be responsible for the difficulty in finding clean targets for therapeutics in this space, and for limited reproducibility. It is likely that this complex target responds differently to drugs affecting different aspects of the cascade, as well as to different drug doses. For example, tumor necrosis factor alpha (TNFα), one of the major pro-inflammatory mediators in this cascade, can have divergent effects at different doses due to differences in activation of its two canonical receptors, TNFR1 and TNFR2 (*TNFRSF1A and 1B)* [8]. Minocycline, methylprednisolone, and other 'anti-inflammatory' therapies also have pleiotropic effects on multiple signaling pathways, and their efficacy in preclinical treatments for SCI has been variable[9-13]. The complex nature of these drugs' actions limits reproducibility of these findings, threatening the predictive potential of preclinical SCI research[14-16]. In the complex tissue microenvironment of the injured CNS, drugs with specific mechanisms of action often lack the breadth of efficacy required to improve behavioral function. Further, the arbitrary selection of a single *a priori* primary outcome metric may lead to a narrow and often-inadequate view of complex disease syndromes where multiple factors contribute to pathogenesis. Focusing on a single univariate outcome metric can thus lead to inaccurate assessments, wasted resources, and failed clinical trials[17]. Improved data integration and multivariate analytics offer opportunities to improve efficacy-testing[18-21] and improve precision medicine for CNS trauma[22].

Here, we used large-scale data-driven discovery techniques to extract syndromic information from complex SCI outcomes data across a series of experiments on neuroinflammatory targets. These data were sequentially obtained in a series of five independent studies that tested promising drugs with reputed anti-inflammatory properties (see **Supplemental Table 1**). We reasoned that combining these studies into an omnibus analytic would provide useful multivariate outcome measures that would leverage variability of the combined large-n dataset to optimize detection of potential treatments and targets. We first performed multidimensional data-curation/integration to incorporate ensemble information from preclinical health records, histology, and behavioral function from 5 different unpublished, blinded preclinical neuroinflammation trials performed over 10 years in our laboratories[23]. We then subjected this high-content data to topological data analysis (TDA) for data-driven discovery, pattern-detection, and dimensionality-reduction[21,24] (**Fig. 1**). This approach was used in a prior *post hoc* analysis of historic VISION-SCI data derived from the multicenter animal spinal cord injury study (MASCIS, see[25]) and allowed us to discover latent predictors of outcome that characterize the entire SCI syndrome as an integrated data system. In that study, we discovered potent predictors of outcome related to physiological measures during SCI induction, and less predictive, but significant, drug effects that had not been found in univariate analyses. When applying TDA to our integrated neuroinflammation dataset, results revealed that only one of the anti-inflammatory interventions tested, intrathecal delivery of a soluble TNF receptor 1 (sTNFR1), yielded a consistent multidimensional benefit across the SCI syndromic space characterized by the TDA network topology.

The beneficial effect of sTNFR1 was discovered by first mapping the multidimensional syndrome across the range of biomechanically-graded experimental cervical SCI severities in the VISION-SCI data commons[23,25] (**Fig.1a-e**). Changing the filter to code for degree of recovery revealed a subset of uniformly moderate injury severities with unexpected gradation in functional recovery after cervical SCI. Changing the filter to depict variations in histopathological outcome

measures revealed that the unusual recovery in these moderate injuries was not attributable to lesion size or white matter sparing. We then asked what conditions were associated with remarkable recovery, and discovered a correspondence between higher measures of behavioral improvement and the dose-response function from a blinded randomized preclinical trial of single bolus intrathecal sTNFR1 delivered to the cervical cord immediately after SCI unilateral contusion (**Fig. 1f**). Thus, in the heat map of the network shown in **Fig. 1h**, more animals from the vehicle group were located within the region of the network that matched poor forelimb recovery, while rats that received sTNFR1 i.t. were concentrated in nodes that had higher performance values in paw preference and grooming (**Fig. 1g**). No other similar relationships were found between drug treatment groups (minocycline, ciclopirox, methylprednisolone, DMSO) and recovery, although each of these had been identified in at least one study as showing efficacy in preclinical SCI[9,12,26]. The sTNFR1 effects appeared to be independent of gross measures of lesion size, white matter and gray matter sparing, or motor neuron numbers. Findings were confirmed by univariate analysis of each outcome; but importantly, none of those independent univariate analyses considered the variability of outcomes in the context of the whole ensemble of treatments and injury variables. Thus, TDA of the combined data from multiple studies appears to be useful in parsing out efficacy and identifying therapeutic promise in combined studies where multiple manipulations and outcomes can be examined in the aggregate.

The TDA showed a pattern suggesting that sTNFR1 had a unique effect on outcomes of combined variables, but did not provide a quantification of that effect. We therefore used the entire combined dataset of prior hemicontusion studies from our lab and applied principal component analysis (PCA) in order to evaluate effects of drug and the relative contribution of multivariables to each syndromic metric[27]. PC1 revealed significant loadings from multiple measures related to both neurological recovery and lesion size, accounting for 27.1% variance (**fig. 1i)**. We then assigned z-scores for this PC for each rat in the sTNFR1 immediate delivery cohort and used analysis of variance to test for significant dose effects. PC1 showed a highly

significant treatment effect, a quadratic contrast indicating an inverted U-shaped dose response function (ANOVA, $p < 0.05$; **Fig. 1j**). This analysis thus indicates that the aggregate syndromic metric PC1, derived from a large population of rats with SCI with and without drug treatment, was improved by sTNFR1 in a dose-dependent manner. Separate univariate analyses of neurological outcome measures, lesion volumes, and motor neuron sparing, revealed significant effects on forelimb function, but not on lesion measures (data not shown). These results suggest that immediate sTNFR1 i.t. treatment can affect long-term neurological outcomes.

Data-driven discovery of the sTNFR1 dose-dependent benefit was accomplished using a dataset with only limited lesion-related histopathological outcome measures, and neither the TDA nor the syndromic PCA detected a clear relationship between spared tissue and neurological function, perhaps implicating more subtle aspects of recovery (e.g. 'plasticity'). While this result was promising, we recognized that the effects of immediate application needed to be extended to later time points if these results were to be relevant to developing therapies. Thorough exploration of time and dose-response variations with studies of long-term outcome is time and effort intensive, so we looked for early biological indices that might predict long-term outcome. We hypothesized that early neuroinflammation (NI) would be correlated with neurological outcomes, and early markers of NI could be used to test for acute effects of sTNFR1 that might translate into long term neurological improvements. Thus, we examined the effects of delayed (90 min post-injury) sTNFR1 on the early production of TNFα and related cytokines, as well as the time course of microglial activation and macrophage invasion over the first week after injury[1] in a series of experiments. SCI produced a rapid increase in TNFα, IL1β and IL-6 protein at 3 hrs after injury, with return toward baseline levels at 24 hrs. Treatment with sTNFR1 decreased the level of TNFα at 3 hours, but did not significantly affect IL-1B or Il-6 (**Fig. 2a-c)**. Microglial/macrophage 'activation' followed, with a protracted development of ED1+ and Iba1+ staining intensity over the first week after SCI (**Fig. 2d, g, j and m,** ANOVA, sham vs. vehicle, $p < 0.05$), as reported for

other SCI models. Treatment with sTNFR1 90 minutes after injury significantly reduced ED-1+ expression at both 24 hours (**Fig. 2f,** ANOVA, vehicle vs. sTNFR1, $p < 0.05$) and 7 days post injury (**Fig. 2i**, ANOVA, vehicle vs. sTNFR1, $p < 0.05$), and Iba1+ expression at 7 days post injury (**Fig. 2o**, ANOVA, $p < 0.05$).

Delayed sTNFR1 treatment at 90 minutes was chosen first because the literature and our preliminary data showed that TNFα was significantly increased at this time point, but returned to normal within several hours. Microarray PCR data showed substantial reversal of the inflammatory response at 3 hours as well (**Supplemental Figure 1**). Thus, the same dose of sTNFR1 that was effective when given immediately after SCI also had dramatic biological effects on neuroinflammation when delayed by 90 minutes.

We next used RNAseq to further examine the effect of sTNFR1 on the injured cord at the molecular level, using 3 groups of rats (Sham SCI, SCI+BSA Vehicle, SCI+sTNFR1, n=5 per group). Differential gene expression analysis revealed more than 5,000 genes induced upon SCI (Sham vs. BSA comparison) and 295 genes that were significantly up- or down-regulated after sTNFR1 injection (BSA vs. sTNFR1 comparison; adjusted p value < 0.05, **Fig. 3a**). A Gene Ontology enrichment analysis (**Fig. 3b**) showed that immune/inflammation-related functions were highly enriched as expected. Ninety-five of the 295 genes belong to the enriched inflammation-related gene ontologies (**Fig. 3b; Supplemental Table 2**). Next, we performed genome-wide gene co-expression network analysis, an unsupervised approach to identify groups of genes with similar expression patterns that capture a substantial amount of overall expression variation[28,29]. Each module was summarized by its first principal component (*co-expression module eigengene,* **Fig. 3c**), and the association strength of each gene with each module (k_{ME}) was determined by correlating its expression pattern with each module eigengene**.**

Applying gene co-expression network analysis reduced the dimensionality of our dataset by more than 3 orders of magnitude and revealed 10 gene modules that were subsequently examined with respect to treatment condition (**Fig. 3c**). In 2 of these modules (arbitrarily

designated M5 and M6), the SCI+Vehicle group changed its transcriptional phenotype in comparison to the Sham group, and upon sTNFR1 treatment a significant reversion of that phenotype was observed (ANOVA, $p < 0.01$; **Fig. 3d**). The eigengenes and top genes for these two modules, which best exemplified the therapeutic effect of sTNFR1, are illustrated in **Fig. 3e and f**. This transcriptomic approach confirms the effect of sTNFR1 treatment on SCI and highlights specific gene networks that are directly or indirectly regulated by TNFα and will be the main targets for intervention in future studies.

Finally, behavioral measures of gross and fine forelimb recovery were assessed over the course of 6 weeks post-SCI, as well as histological analysis of cell sparing, lesion size, and neuroinflammation markers. **Figure 4** shows the long-term outcomes from groups of rats receiving 90-min delayed sTNFR1 vs BSA vehicle controls. Each of the forelimb outcome measures was significantly better over 6 weeks in the sTNFR1-treated group (ANOVA, $p < 0.05$, **Fig. 4a-b**). There was a significant decrease in OX-42 staining 6 weeks after SCI in the sTNFR1-treated group compared to vehicle (ANOVA, $p < 0.05$, **Fig. 4c-d**). Therefore, the degree of persistent neuroinflammation may be a factor in determining behavioral outcome, and acute bolus treatment with sTNFR1 that affects early TNFα production/expression appears to have a lasting effect on the development of neuroinflammation and on neurobehavioral outcomes[30]. Mironets et al (2018) have provided additional evidence for a critical role for sTNF signaling in the production of long term neurological and immune dysfunction after thoracic SCI[31]. Thus, multiple approaches and experiments lead to the conclusion that modulation of the sTNF signaling offers a viable approach to therapeutic treatments for SCI. Accordingly, the advanced TDA and transcriptomics analyses we employed to identify sTNFR1 as an effective delayed treatment for cervical SCI may be useful in streamlining the evaluation of the pharmacological treatments aimed at improving post CNS recovery of function. In addition, the ability to identify novel gene expression modules

that associate with better outcomes is likely to be useful for identifying novel therapeutic targets that could be tested in a variety of preclinical neurotrauma models.

REFERENCES

1. Popovich, P. & McTigue, D. Damage control in the nervous system: beware the immune system in spinal cord injury. *Nat. Med.* **15,** 736–737 (2009).
2. Donnelly, D. J. & Popovich, P. G. Inflammation and its role in neuroprotection, axonal regeneration and functional recovery after spinal cord injury. *Exp. Neurol.* **209,** 378–388 (2008).
3. Nielson, J. L. *et al.* Topological data analysis for discovery in preclinical spinal cord injury and traumatic brain injury. *Nat Commun* **6,** 8581 (2015).
4. Torres-Espín, A., Forero, J., Fenrich, K. K., Brain, A. L.-O.2018. Eliciting inflammation enables successful rehabilitative training in chronic spinal cord injury. *academic.oup.com*
5. Alexander, J. K. & Popovich, P. G. Neuroinflammation in spinal cord injury: therapeutic targets for neuroprotection and regeneration. *Prog. Brain Res.* **175,** 125–137 (2009).
6. Yong, H. Y. F., Rawji, K. S., Ghorbani, S., Xue, M. & Yong, V. W. The benefits of neuroinflammation for the repair of the injured central nervous system. *Cell. Mol. Immunol.* **16,** 540–546 (2019).
7. Gensel, J. C., Kigerl, K. A., Mandrekar-Colucci, S. S., Gaudet, A. D. & Popovich, P. G. Achieving CNS axon regeneration by manipulating convergent neuro-immune signaling. *Cell Tissue Res.* **349,** 201–213 (2012).
8. Barnum, C. J. & Tansey, M. G. The duality of TNF signaling outcomes in the brain: potential mechanisms? *Exp. Neurol.* **229,** 198–200 (2011).
9. Lee, S. M. *et al.* Minocycline Reduces Cell Death and Improves Functional Recovery after Traumatic Spinal Cord Injury in the Rat. *http://dx.doi.org/10.1089/08977150152693764* **20,** 1017–1027 (2004).
10. Pinzon, A. *et al.* A re-assessment of minocycline as a neuroprotective agent in a rat spinal cord contusion model. *Brain Res.* **1243,** 146–151 (2008).
11. Lee, J. H. T. *et al.* Lack of neuroprotective effects of simvastatin and minocycline in a model of cervical spinal cord injury. *Exp. Neurol.* **225,** 219–230 (2010).
12. Constantini, S. & Young, W. The effects of methylprednisolone and the ganglioside GM1 on acute spinal cord injury in rats. *J. Neurosurg.* **80,** 97–111 (1994).
13. Oudega, M., Vargas, C. G., Weber, A. B., Kleitman, N. & Bunge, M. B. Long-term effects of methylprednisolone following transection of adult rat spinal cord. *Eur. J. Neurosci.* **11,** 2453–2464 (1999).
14. Landis, S. C. *et al.* A call for transparent reporting to optimize the predictive value of preclinical research. *Nature* **490,** 187–191 (2012).
15. Collins, F. S. & Tabak, L. A. Policy: NIH plans to enhance reproducibility. *Nature* **505,** 612–613 (2014).
16. Steward, O. & Balice-Gordon, R. Rigor or mortis: best practices for preclinical research in neuroscience. *Neuron* **84,** 572–581 (2014).
17. Chan, A.-W. *et al.* Increasing value and reducing waste: addressing inaccessible research. *Lancet* **383,** 257–266 (2014).
18. Glasziou, P. P., Chalmers, I., Green, S. & Michie, S. Intervention synthesis: a missing link between a systematic review and practical treatment(s). *PLOS Medicine* **11,** e1001690 (2014).

19. Ioannidis, J. P. A. How to make more published research true. *PLOS Medicine* **11,** e1001747 (2014).
20. Huie, J. R., Almeida, C. A. & Ferguson, A. R. Neurotrauma as a big-data problem. *Curr. Opin. Neurol.* **31,** 702–708 (2018).
21. Ferguson, A. R., Nielson, J. L., Cragin, M. H., Bandrowski, A. E. & Martone, M. E. Big data from small data: data-sharing in the 'long tail' of neuroscience. *Nat. Neurosci.* **17,** 1442–1447 (2014).
22. Manley, G. T. & Maas, A. I. R. Traumatic brain injury: an international knowledge-based approach. *JAMA* **310,** 473–474 (2013).
23. Nielson, J. L. *et al.* Development of a database for translational spinal cord injury research. *J. Neurotrauma* **31,** 1789–1799 (2014).
24. Cunningham, J. P. & Yu, B. M. Dimensionality reduction for large-scale neural recordings. *Nat. Neurosci.* **17,** 1500–1509 (2014).
25. Nielson, J. L. *et al.* Topological data analysis for discovery in preclinical spinal cord injury and traumatic brain injury. *Nat Commun* **6,** 8581 (2015).
26. Zileli, M., Ovül, I. & Dalbasti, T. Effects of methyl prednisolone, dimethyl sulphoxide and naloxone in experimental spinal cord injuries in rats. *Neurol. Res.* **10,** 232–235 (1988).
27. Ferguson, A. R. *et al.* Derivation of Multivariate Syndromic Outcome Metrics for Consistent Testing across Multiple Models of Cervical Spinal Cord Injury in Rats. *PLoS ONE* **8,** e59712 (2013).
28. Zhang, B., biology, S. H. A. I. G. A. M.2005. A general framework for weighted gene co-expression network analysis. *degruyter.com*
29. Kelley, K. W., Nakao-Inoue, H., Molofsky, A. V. & Oldham, M. C. Variation among intact tissue samples reveals the core transcriptional features of human CNS cell classes. *Nat. Neurosci.* **21,** 1171–1184 (2018).
30. Huie, J. R. *et al.* Glial tumor necrosis factor alpha (TNFα) generates metaplastic inhibition of spinal learning. *PLoS ONE* **7,** e39751 (2012).
31. Mironets, E. *et al.* Soluble TNFα Signaling within the Spinal Cord Contributes to the Development of Autonomic Dysreflexia and Ensuing Vascular and Immune Dysfunction after Spinal Cord Injury. *J. Neurosci.* **38,** 4146–4162 (2018).
32. Gensel, J. C. *et al.* Behavioral and histological characterization of unilateral cervical spinal cord contusion injury in rats. *http://dx.doi.org/10.1089/08977150152693764* **23,** 36–54 (2006).
33. Irvine, K.-A. *et al.* A novel method for assessing proximal and distal forelimb function in the rat: the Irvine, Beatties and Bresnahan (IBB) forelimb scale. *J Vis Exp* (2010). doi:10.3791/2246
34. Livak, K. J. & Schmittgen, T. D. Analysis of relative gene expression data using real-time quantitative PCR and the 2(-Delta Delta C(T)) Method. *Methods* **25,** 402–408 (2001).
35. Oldham, M. C., Langfelder, P. & Horvath, S. Network methods for describing sample relationships in genomic datasets: application to Huntington's disease. *BMC Syst Biol* **6,** 63–18 (2012).
36. Johnson, W. E., Li, C. & Rabinovic, A. Adjusting batch effects in microarray expression data using empirical Bayes methods. *Biostatistics* **8,** 118–127 (2007).
37. Leek, J. T., Johnson, W. E., Parker, H. S., Jaffe, A. E.2012. The sva package for removing batch effects and other unwanted variation in high-throughput experiments. *academic.oup.com*
38. Langfelder, P. & Horvath, S. WGCNA: an R package for weighted correlation network analysis. *BMC Bioinformatics 2008 9:1* **9,** 1–13 (2008).
39. Horvath, S. & Dong, J. Geometric Interpretation of Gene Coexpression Network Analysis. *PLOS Computational Biology* **4,** e1000117 (2008).

40. Kaiser, H. F. (1960). The Application of Electronic Computers to Factor Analysis: *Educational and Psychological Measurement*. https://doi.org/10.1177/001316446002000116
41. Cattell, R. B. The Scree Test For The Number Of Factors. *Multivariate Behav Res* **1,** 245–276 (1966).
42. Hogarty, K. Y., Hines, C. V., Kromrey, J. D., Ferron, J. M. & Mumford, K. R. The Quality of Factor Solutions in Exploratory Factor Analysis: The Influence of Sample Size, Communality, and Overdetermination:. *Educational and Psychological Measurement* **65,** 202–226 (2016).

ONLINE METHODS

Animals. Female Long-Evans hooded rats (Simonsen Laboratories, Gilroy, CA, USA) with a mean weight of 230 g and mean age of 77 days were used in this study. Rats were triple-housed in plastic cages, maintained on a 12-hour light/dark cycle, and had access to food and water *ad libitum*. All experiments were approved by the Institutional Laboratory Animal Care and Use Committee of the University of California at San Francisco and were performed in compliance with NIH guidelines and recommendations. Surgical procedures were carried out under aseptic conditions, during which animals were kept under deep anesthesia induced and maintained by isoflurane inhalation (IsoFlow, Abbott Laboratories, North Chicago, IL, USA; 2-3%). Anesthetic plane was monitored by testing withdrawal to foot pinch. Cefazolin (Ancef, Novation, LCC, Irving, TX) 25 mg/kg, was administered prior to surgery and for 3 days postoperatively (for chronic injured subjects). Lacrilube ophthalmic ointment (Allergan Pharmaceuticals, Irvine, CA, USA) was applied to the eyes prior to surgery and body temperature was monitored using a rectal thermal probe and maintained at 37.5 $\pm$ 0.5 C using a heating pad.

Unilateral cervical spinal contusion injury. Spinal cord injury was delivered as described previously[30]. Briefly, a dorsal, midline skin incision was made, the skin dissected, and the trapezius muscle was cut just lateral to the midline from C1/2 to T2. Muscle layers were dissected

to expose C3-T1 spinous processes. A dorsal laminectomy was then performed at C5 to expose the spinal cord. Contusion injury was produced using an Infinite Horizons Impactor (Precision Systems, Fairfax, VA, USA) fitted with a 2mm impactor tip that was centered over the right side of the C5 spinal segment. Impactor was computer-controlled to consistently impact the spinal cord at a force of 75 kilodynes. After injury, trapezius muscle was sutured and skin incision closed with wound clips. The analgesic buprenorphine (0.05 mg/kg), and the antibiotic Cefazolin (50mg/kg, Henry Schein, Melville, NY) were administered, and the animal recovered overnight in an incubator (Thermocare Intensive Care Unit with Dome Cover; Thermocare, Inclined Village, NV). All animals were inspected daily for wound healing, weight loss, dehydration, autophagia and discomfort. Appropriate veterinary care was provided when needed.

Drug Delivery. Human recombinant soluble TNF receptor 1 (sTNFαR1; R&D systems) was delivered by way of an intrathecal cannula (30 cm, PE-10, sterilized with 95% ethanol and prefilled with sterile 0.2% BSA vehicle) that was placed in the cisterna magna and threaded 1 cm caudally into the subarachnoid space until it was visible under the dura within the laminectomy site at C4/5, and then positioned so that it was directly rostral to the laminectomy window. The cannula tip was positioned over the hemicord, contralateral to the target site for unilateral contusion. The cannula was fixed in place using two bilateral finger trap sutures into the sternohyoid muscles. Subjects were then placed in the Inifinite Horizons impact device and the external cannula tip was heat flanged and then connected to a 10 µl Hamilton syringe filled with sterile sTNFR1 solution or vehicle in a blinded, randomized fashion. Immediately following contusion injury, drug was delivered intrathecally over 5 minutes followed by a 20µL vehicle (sterile, 0.2% BSA) flush over 10 minutes. Following drug delivery, finger trap sutures were removed, the cannula was carefully withdrawn, and the surgery site was closed using standard surgical procedures[32,33]. Subjects were carefully monitored post-operatively for signs of bilateral deficits, indicating potential damage by the cannulization procedures. Ciclopirox was delivered

subcutaneously at a concentration of 10 mg/kg. The vehicle control for the ciclopirox study was dimethyl sulfoxide (DMSO). DMSO was delivered subcutaneously at a concentration of 1 mg/kg. Methylprednisolone was given intravenously at a concentration of 30 mg/kg. Minocycline was delivered intraperitoneally at a concentration of 45 mg/kg.

Paw Preference Test. Animals were placed in a clear plastic cylinder that is situated in mirrored corner, so that the animal can be viewed from all angles. Animals are filmed on a digital camera while they explore the cylinder for 3 minutes. Slow motion high-definition playback of each session allows a rater who is blind to condition to record each time a weight-supported placement is made on the cylinder wall by either the left forepaw alone, right forepaw alone, or both. A “left” or “right” count was given if the other limb did not contact the side of the cylinder within 0.5 sec of the initial placement. A “both” count was given if both forepaws were placed on the cylinder within 0.5 sec of each other. During lateral exploration, a “both” score was also given for each two step “walking” sequence, during which both paws changed position on the cylinder wall. If one paw remained in place while the other was placed on different parts of the cylinder, a count was not given until the anchored paw was lifted.

Grooming Test. An assessment of stereotypical grooming behavior was adapted for use in cervical model of SCI by Gensel et al., and used to determine recovery of forelimb range of motion[32]. Cool tap water was applied with gauze to the animal’s head and back, and then the animal was placed in a clear plastic cylinder with mirrors on either side so that the animal could be observed from all angles. Grooming activity was recorded with a digital video camera from the onset of grooming through at least 2 grooming sequences. Slow motion high-definition playback was used to score each forelimb independently, using a 6-point scoring system as follows: 0 indicates the animal is unable to make contact with the forepaw to any part of the face or head; 1 indicates the animal’s forepaw can make contact with the underside of the chin and/or mouth

area; 2 indicates the animal's forepaw can make contact with the area between the nose and eyes, but not the eyes; 3 indicates the animal's forepaw can make contact with the eyes and the area up to, but not including, the front of the ears; 4 indicates the animal's forepaw can make contact with the ears, but not the area of the head behind the ears; 5 indicates the animal's forepaw can make contact with the area of the head behind the ears. Animals were tested at 2, 7, 14, 21, 28, 35, and 42 days after injury.

Irvine, Beatties, Bresnahan (IBB) forelimb rating scale

Fine forelimb function was assessed using a cereal eating test as described in Irvine et al. [33]. Animals were individually placed in their home cages and given doughnut- and spherical-shaped pieces of cereal, and eating was filmed with a digital video camera. Slow motion high-definition playback was used to evaluate forepaw use. Evaluation was made using a standardized scoring of forelimb behaviors while eating (e.g. joint position, object support, digit movement, and grasping technique). An IBB score was assigned using the 10 point (0-9) ordinal scale for each shape.

Histological preparation. Animals were perfused through the left ventricle of the heart with 4% paraformaldehyde under deep anesthesia with pentobarbital. The cords were removed and post-fixed in 4% paraformaldehyde for 2 hr and then cryoprotected in PBS containing 30% sucrose. A 2 mm block containing the lesion epicenter was then incubated in 100% OCT for 2 hr and then mounted in a cryomold (filled with OCT) in coronal orientation and rapidly frozen using dry ice. The blocks were stored at –80°C until sectioning. The cords were cut coronally at 20 um and every section was retained and mounted. Sections were stained with Luxol fast blue for myelin/white matter integrity and counterstained with Cresyl violet or for cell body assessment.

Sparing at lesion epicenter: A camera lucida drawing of the section with the largest extent of lesion (the lesion epicenter) was made outlining intact gray and white matter, and the lesion. Pixel counts from digitized drawings in Adobe Photoshop 5.5 (Adobe Systems Inc., San Jose, CA) were used to determine the area of spared tissue for both hemi-cords at the lesion center. The percent sparing for the ipsilateral hemi-cord was determined by dividing the total spared ipsilateral tissue area, spared white matter tissue area, or spared gray matter tissue area, by the same measure from the contralateral hemi-cord [(ipsilateral spared tissue area/contralateral spared tissue area)x100]. This normalized within subjects and corrected for any biological differences in spinal cord size or tissue preparation.

Immunohistochemistry. Fixed spinal tissue sections were blocked and permeabilized for 1 h with 10% normal donkey serum and 0.3% Triton X-100. The sections were then incubated overnight at room temperature (RT) with mouse monoclonal antibody for ED1 (1:300; Bio-Rad Laboratories, Hercules, CA, USA) and Iba-1 (1:500; Fujifilm Wako Chemical. Richmond, VA, USA). After washing with phosphate-buffered saline (PBS) 2 ml, the slides were incubated for 1 h at RT with fluorescent (Alexa 488 and 594) donkey anti-mouse secondary antibody (1:1000; Life Technologies, Carlsbad, CA, USA). The slides were briefly rinsed with PBS 2 ml and coverslipped with VECTASHIELD ® containing 40,6-diamidino-2-phenylindole (Vector Laboratories, Burlingame, CA, USA). The stained spinal tissue sections were photographed using the BioRevo fluorescence microscope BZ-9000 Generation II (Keyence, Itasca, IL, USA). Fluorescence was measured using BZ-9000 Generation II analyzer (Keyence) and analyzed by NIH ImageJ. Proportional area measurements were acquired by adjusting the thresholds of stained sections in image J and ratio of immunoreactive area to the section area was calculated. Every eighth section of the spinal cord was analyzed for a distance of up to 5 mm in the rostral and caudal directions from lesion center.

OX-42 staining. Slides were first washed 2 x 5 min in Tris-buffered phosphate (TBS) with Triton X-100 (0.025%). Slides were then blocked in 10% normal goat serum with 1% bovine serum albumin (BSA) in TBS for 2 h at room temperature. Primary antibody (anti-OX-42, 1:500, Abcam) was then added, and incubated overnight at 4^{o} C. Slides were then rinsed 2 x 5 min in TBS+ Triton X-100, and incubated in horseradish peroxidase (H_2O_2) in TBS with 1% BSA for 15 min. To visualize reaction, DAB chromagen with nickel enhancement was added, followed by dehydration and tissue clearing.

OX-42 quantification. As specific microglia cell counting is often obfuscated by clustered and overlapping cells, quantification of OX-42 expression was performed by calculating area of positive staining on the injured hemisphere, and correcting by the contralateral uninjured hemisphere. Threshold for positive staining was determined using MetaMorph image analysis software. Briefly, an image analysis macro script was written to first set the relative white balance for each image, then determine the ratio between number of pixels above threshold and the total number of pixels in the area. This process was repeated for both ipsi- and contralateral sides of the spinal cord, and the final percentage of OX-42 expression was formulated by dividing pixels above threshold on ipsilateral side by pixels above threshold on contralateral side.

Luminex multiplex cytokine assays. Total cellular proteins were prepared from spinal cord tissue. Aliquots were analyzed for inflammatory cytokines, with Luminex xMAP multiplexing technology (Luminex Corp., Austin, TX). Spinal cord protein specimens were prepared for analysis in a 96-well plate utilizing a custom 7-cytokine Milliplex MAP Rat Cytokine/Chemokine Magnetic Bead Panel (RECYTMAG-65K, Millipore Corp., Billerica, MA) following the kit-specific protocols provided by Millipore. Analytes were quantified using a Magpix analytical test instrument, which utilizes xMAP technology (Luminex Corp., Austin, TX), and xPONENT 4.2 software (Luminex Corp.). xMAP technology uses fluorescent-coded magnetic microspheres coated with analyte-

specific capture antibodies to simultaneously measure multiple analytes in a specimen. After microspheres have captured the analytes, a biotinylated detection antibody binds to that complex. Streptavidin PE then attaches as a reporter molecule. Inside the instrument, magnetic beads are held in a monolayer by a magnet, where two LEDs are used to excite the internal microsphere dye and the dye of the reporter molecule, respectively. A CCD camera captures these images, which are then analyzed by Milliplex Analyst software (Millipore).

Assay of inflammatory chemokine and cytokine gene expression. Acute injured animals (3 hours post-injury) were deeply anesthetized with 5% isoflurane. Animals were given a brief intracardiac saline perfusion, and then a section of spinal cord (centered rostrocaudally around the lesion) were removed, flash-frozen in isopentane, and then stored at -80 C. To assess changes within and between subjects, cords were split on the midline, to produce injured and uninjured hemicords. RNA from spinal hemicords were extracted and purified using an RNEasy Lipid Minikit (Qiagen) and RNA concentration was quantified using a Biomate 3 spectrophotometer (Thermo Scientific) set to read absorbance at 260 nanometers. Equal amounts of RNA per hemicord were subjected to reverse transcriptase reaction (RT2 First Strand Kit, SABiosceinces) to yield cDNA. Equal volumes of cDNA for each hemicord were pooled by condition, and subjected to PCR amplification using a commercially available multitarget Inflammatory cytokine/chemokine array (Qiagen). One array was used per pooled condition. PCR data were then normalized to housekeeping genes and fold changes in mRNA expression between conditions were calculated using the Delta-Delta Ct Method[34].

RNA extraction. 1 cm of hemicord was homogenized in 1 ml of TRIZOL solution (Thermo Fischer #15596018) and subsequently total RNA was extracted using the manufacturer's protocol. RNA was purified one additional time using 3M sodium acetate.

Library preparation. 1 µg of extracted RNA was used for the library synthesis. DNA library was synthesized using Illumina's TruSeq Stranded Total RNA with Ribo-Zero Globin and by following the manufacturer's instructions. Libraries were then quantified and tested for proper fragmentation using the 2100 Agilent bioanalyzer and the Agilent DNA 1000 kit (Agilent # 5067-1504).

RNAseq. Samples were sequenced on Illumina's HiSeq 4000 aiming for 40 million single-ended reads per sample.

Bioinformatic analysis. We used the software packages Scythe and Sickle to trim reads as necessary to achieve maximum quality. We aligned the trimmed reads against the rat genome and transcriptome using the TopHat2/Bowtie2 software. After read alignment, we used the featureCount function in R to get the raw counts of every transcript in our samples. Data were examined for outliers using the SampleNetwork R function[35] and batch effects were corrected using the ComBat function[36] of the sva package in R[37]. Unsupervised gene co-expression network analysis[28,29] was performed using a four-step approach. First, pairwise biweight midcorrelations (bicor) were calculated for all analyzed transcripts over all samples using the bicor function in the WGCNA R package[38]. Second, transcripts were clustered using the flashClust implementation of a hierarchical clustering procedure with complete linkage (minimum cluster size = 12) and 1 – bicor as a distance measure. Third, the resulting dendrogram was cut at a height corresponding to the top 10% of pairwise correlations. Fourth, modules were summarized by their eigengenes[39], defined as the first principal component obtained by singular-value decomposition of the coexpression module, and highly similar modules were merged if the correlations of their module eigengenes exceeded 0.85. This procedure was performed iteratively, such that the pair of modules with the highest correlation (>0.85) was merged first, followed by recalculation of module eigengenes, followed by recalculation of all correlations, until no pairs of modules exceeded the threshold. The WGCNA measure of intramodular connectivity

(k_{ME}) was then calculated for each gene with respect to all modules by correlating its expression pattern across all samples with each module eigengene.

Statistical Analyses. Topological data analysis (TDA) was conducted according to methods previously described[2]. Briefly, TDA uses an ensemble machine learning algorithm to rapidly iterate across subject bins, resampling the metric space and replacing subjects after each sampling. This resampling procedure ultimately arrives at the most stable 'consensus vote' that best represents the multidimensional data shape. The result of this approach is a clustering of subjects ('nodes') and the connections between these clusters ('edges' or lines). Variables and outcomes of interest that were used in the TDA included injury condition, drug condition, behavioral endpoints, and histological endpoints (tissue sparing, lesion size, etc). Heat maps for the color schemes of the flares represent the range of highest values (red) to lowest values (blue) for each respective outcome being visualized.

Principal component analysis was performed by eigenvalue decomposition of the correlation matrix of all outcomes in using the FACTOR subcommand in SPSSv.18. This method extracts PCs that are uncorrelated (orthogonal) partitions of the variance. PCs were retained using 3 criteria: 1) retaining PCs with eigenvalues > 1.0 (Kaiser rule) [40] 2) Scree plot[41], and 3) the over-determination of the factors[42], retaining factors with at least 3 loadings above |.4|. PCs meeting all three criteria were examined and named using loadings above |.4|, thereby accounting for at least 20% of the variance. Visualization of PC loadings was achieved using the syndRomics package in the R statistical software program. To test for univariate effects of drug treatment on principal component scores, protein expression, behavior, and eigenmodule scores, we performed analyses of variance (ANOVA) using the SPSS GLM subcommand or R statistical software. Significant ANOVAs were followed by Tukey's posthocs. To assess dose response we performed an additional polynomial contrast analysis. Significance for all univariate effects was assessed at $p < .05$.

Figure 1.

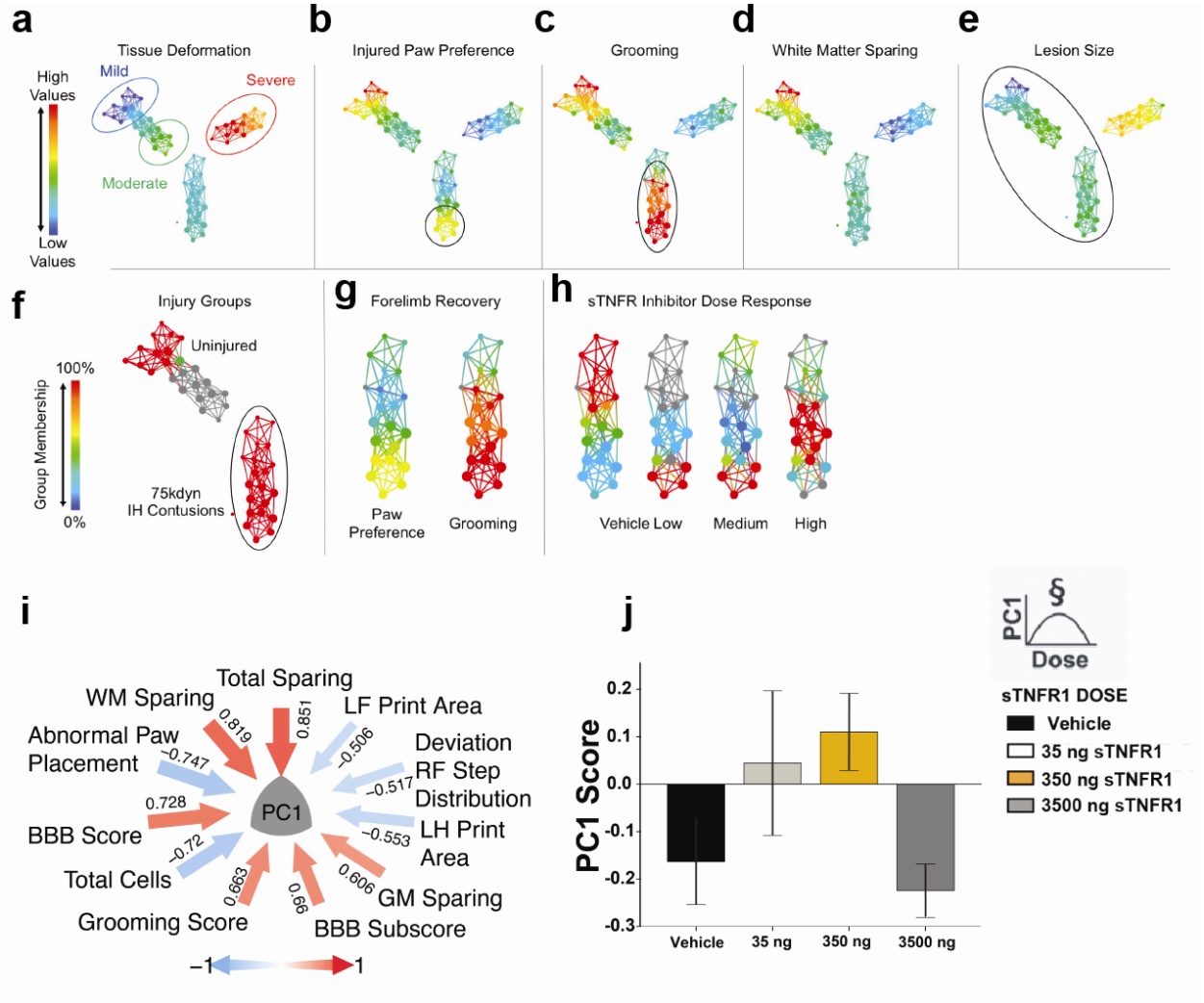

Figure 1. Topological Data Analysis (TDA) identifies sTNFR1 among 5 preclinical trials as effective therapy after SCI. High-content data from 5 previous unpublished preclinical SCI trials were merged and topological data analysis was run in order to extract syndrome-level information. The multidimensional array of outcome measures was mapped to a data topology, with nodes (colored circles) representing clusters of subjects that share similar multivariate patterns, and edges (lines) that represent shared similarities between nodes. TDA on all animals in preclinical drug trials revealed a distinct separation of subjects based on injury severity (a). **b-e,** filtering the topology by different measures reveals how those with moderate injuries have a distinct, non-uniform pattern of recovery (**b**). A robust recovery of forelimb function (black circles, b-c) not dependent on tissue pathology (**d-e**) was observed. Exploration of nodes of interest (black circle, e) revealed they were given the same 75 kdyne IH contusion injury (f), and that the robust forelimb recovery (**g**) was the result of a dose response to sTNFR1 treatment (**h**). Heat maps: high-low for values (**a-e, g**), 100-0% for group membership(**f,h**). Principal components analysis on all hemicontusion data revealed a first principal component (PC1) that explained 27.1% of the total variance in the dataset (**i**). Hypothesis testing for an effect of sTNFR1 on PC1 revealed a significant dose response effect (polynomial contrast), indicating that sTNFR1 treatment has a multivariate effect that is detectable across the syndromic SCI space (**j**). Error bars represent standard error of the mean, * $p < 0.05$.

Figure 2.

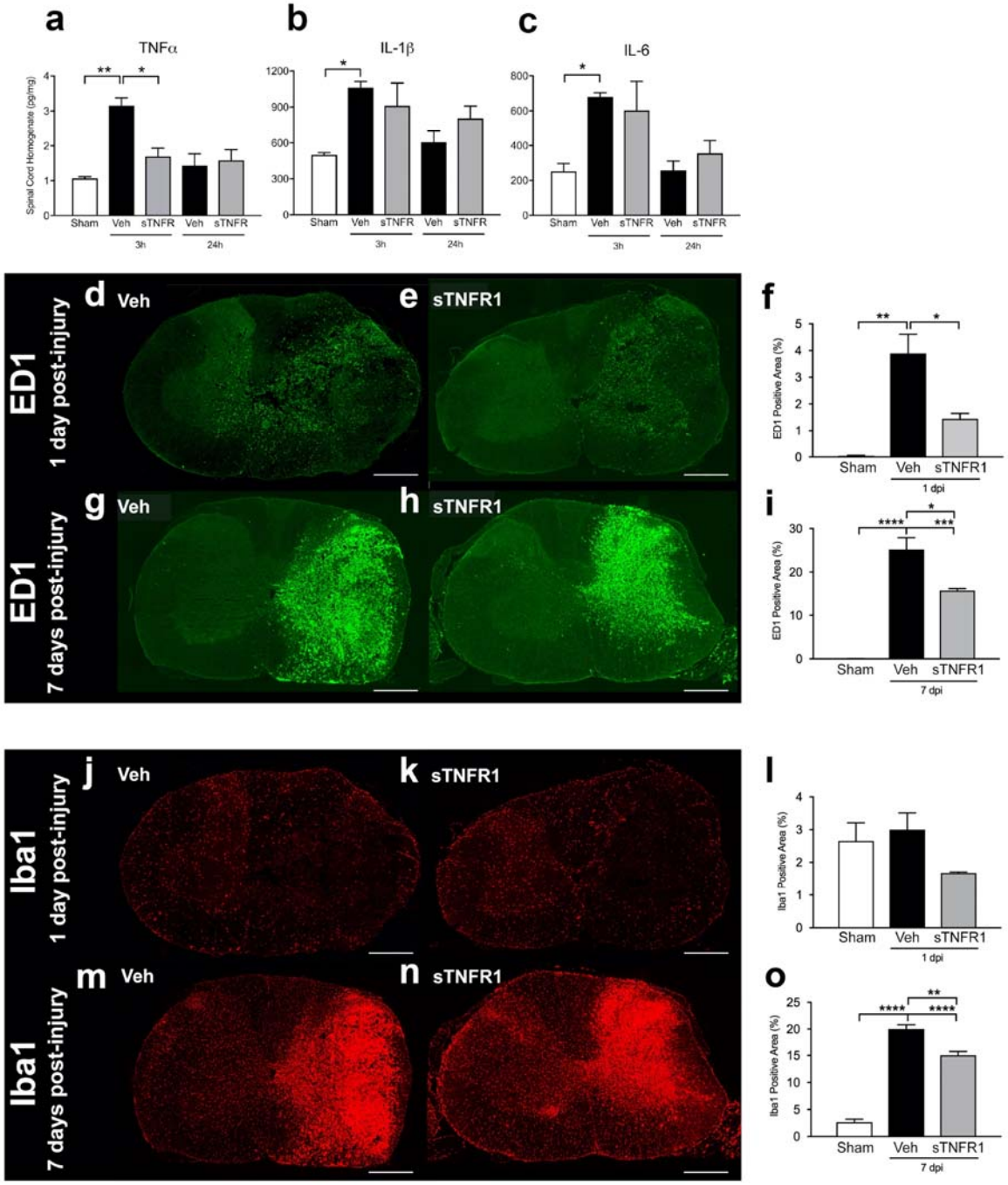

Figure 2. Acute sTNFR1 treatment reduces indicators of neuroinflammation. a-c, Spinal cord injury produces a strong early (3 hr) inflammatory cytokine (TNFα, IL1-β, and Il-6) protein expression. TNFα expression is significantly mitigated by sTNFR1 treatment. **d-e**, Immunohistochemical stain of injured spinal cord shows SCI-induced expression of ED1+ cells at 1 day and 7 days post-injury, and early i.t. sTNFR1 treatment significantly reduces ED1 at both 1 day and 7 days **(f,i). j-n**, Expression of Iba1+ cells following spinal cord injury at 1 day and 7 days post-injury. early i.t. sTNFR1 treatment did not affect Iba1 expression at 1 day post-injury, but did significantly reduce Iba1 expression by 7 days post-injury **(l,o).** Scale bars represent 400 um. Error bars represent standard error of the mean, One-way ANOVA, * $p < 0.05$, ** $p < 0.01$, *** $p < 0.001$, **** $p < 0.0001$.

Figure 3.

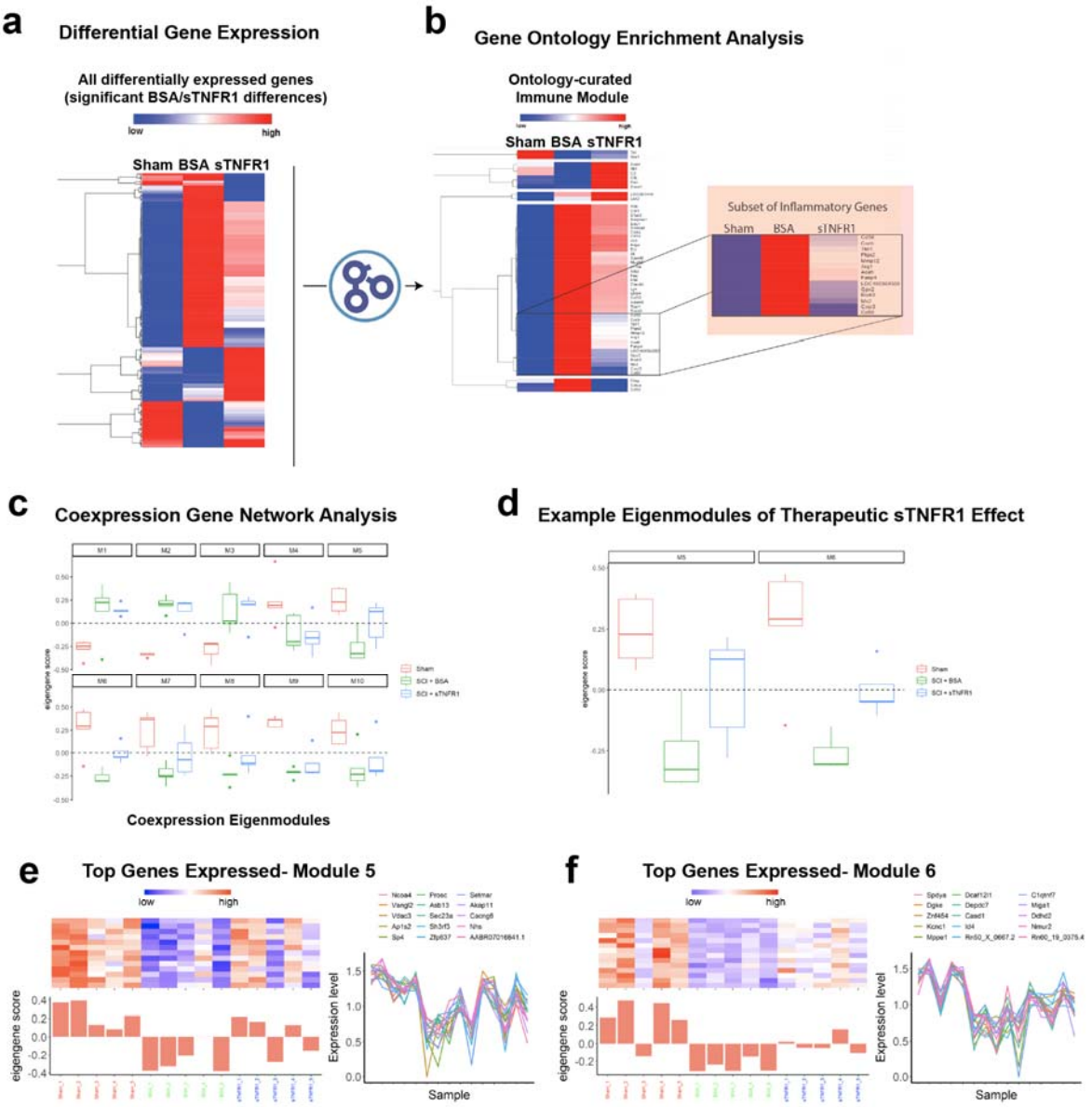

Figure 3. Differential gene expression in response to i.t. sTNFR1 treatment. RNAseq was used to explore the effect of sTNFR1 on the molecular level after SCI. **a,** We identified 295 differentially expressed genes (BSA vs. sTNFR1); 224 of those genes were altered by SCI (and BSA injection) and sTNFR1 administration reversed that change (partially or fully) to bring expression back to the pre-injury levels. **b**, Gene Ontology enrichment analysis was used to discover the processes that were most robustly affected by sTNFR1, revealing predominant inflammation/immune genes that were altered. A closer look at the ontology-curated immune module shows 52 genes to be involved in some capacity in immune and defense responses; sTNFR1 treatment reversed expression levels for a majority of these genes. **c,** Unsupervised gene coexpression network analysis identified 10 modules, which were summarized by their eigengenes and related to treatment effect**. d,** In two modules (M5, M6), sTNFR1 treatment significantly reversed the transcriptional phenotype compared to Sham and BSA vehicle treatment (one-way ANOVA, $p < 0.05$, error bars represent standard error of the mean). **e-f,**

Module eigengenes and genes with the highest k_{ME} values (Pearson correlation to module eigengene) for modules M5 and M6, which best exemplified the therapeutic effect of sTNFR1.

Figure 4.

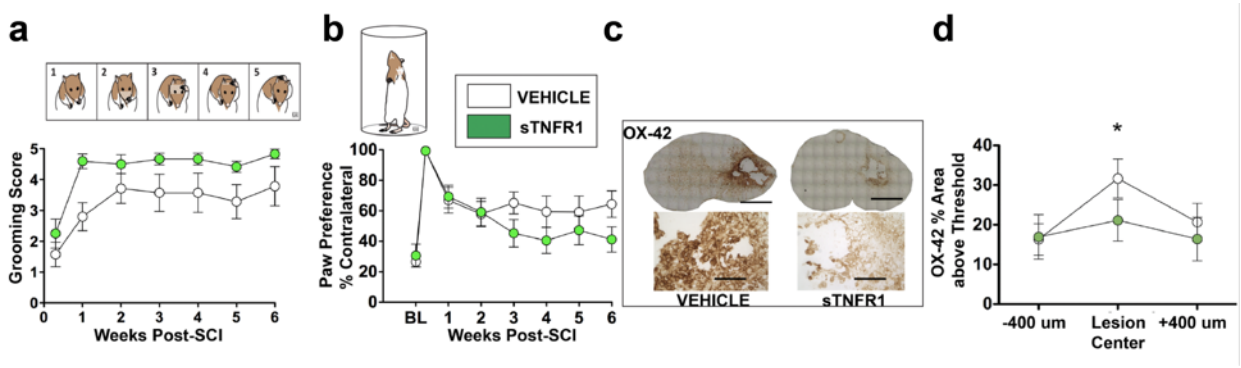

Figure 4. Acute sTNFR1 treatment improves behavioral recovery and mitigates chronic neuroinflammation. Tests of forelimb recovery following unilateral cervical contusion were assessed for 6 weeks post-injury. Subjects that received a single acute i.t. sTNFR1 bolus showed significantly better scores on grooming (**a**) and paw placement (**b**) tests over 6 weeks (Repeated-measures ANOVA, Time x Treatment, $p < 0.05$). Terminal histological assessment of neuroinflammation at 6 weeks post-injury (**c)** show that sTNFR1 treatment significantly reduced OX-42 expression (**d,** ANOVA, $p < 0.05$) indicating that early intervention with sTNFR1 was sufficient to block the development of lasting neuroinflammation. Error bars represent standard error of the mean, * $p < 0.05$.

Study	Drug Delivery	Dose	SCI Model	SCI Severity	SCI Level	Laterality	Number of animals
Methylprednisolone	intravenous	30mg/kg	NYU Impactor	12.5mm drop	C5	Unilateral	10
Minocycline	intraperitoneal	45mg/kg	NYU Impactor	12.5mm drop	C5	Unilateral	11
DMSO	subcutaneous	1mg/kg	IH Impactor	100 kilodyne	C5	Unilateral	12
Ciclopirox	subcutaneous	10mg/kg	IH Impactor	100 kilodyne	C5	Unilateral	8
sTNFR1	intrathecal	0.035-3.5ng	IH Impactor	75 kilodyne	C5	Unilateral	32
Bovine Serum Albumin vehicle	intrathecal	0.002	IH Impactor	75 kilodyne	C5	Unilateral	17

Supplemental Table 1. Anti-inflammatory drug studies. Parameters of drug type and dose for each drug study that was included in the initial data-driven analysis of multivariate treatment effects.

Supplemental Figure 1.

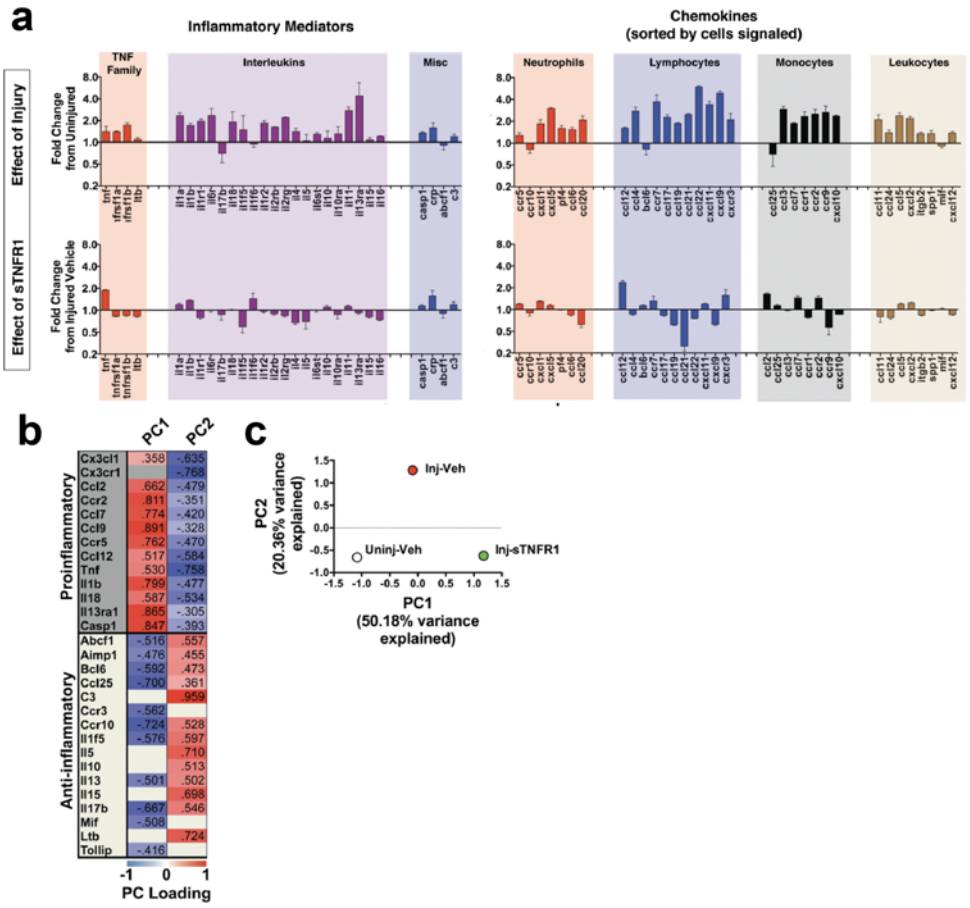

Supplemental Figure 1. Effect of sTNFR1 on inflammatory gene panel. A multiplexed PCR panel of 84 inflammatory genes was used to assess the broad effect of sTNFR1 treatment on neuroinflammation after SCI. sTNFR1 was delivered i.t. 90 minutes after injury, and spinal cord was harvested for PCR 3 hours after injury. **a**, Overall expression levels were increased in the vehicle-treated SCI group, as expressed by fold-change relative to uninjured sham control subjects ("Effect of Injury"). sTNFR1 treatment either dampened or reversed this neuroinflammatory response in the majority of genes tested. ("Effect of sTNFR1"). **b**, Principal components analysis of all gene expression values across all testing groups revealed two principal components that together accounted for 71% of the variance. PC1 was characterized by high positive loadings in classically pro-inflammatory genes, and PC2 was most strongly driven by anti-inflammatory genes. **c,** biplot of the three experimental groups on the PC1 and PC2 axes illustrates the 2 dimensional syndromic space occupied by each experimental condition. sTNFR1 treatment (Inj-sTNFR1) produces an inflammatory profile that is distinct from both injury alone (Inj-Veh) and uninjured controls (Uninj-Veh).

Supplemental Table 2.

GO Term	Description	P-value	FDR q-value	Enrichment	N
GO:0009605	response to external stimulus	8.26E-14	1.29E-09	2.7	17807
GO:0009607	response to biotic stimulus	2.48E-13	1.94E-09	3.44	17807
GO:0043207	response to external biotic stimulus	4.00E-13	2.08E-09	3.46	17807
GO:0080134	regulation of response to stress	4.11E-13	1.61E-09	3.02	17807
GO:0032101	regulation of response to external stimulus	1.45E-12	4.54E-09	3.78	17807
GO:0031347	regulation of defense response	7.21E-12	1.88E-08	4.07	17807
GO:0048518	positive regulation of biological process	1.04E-11	2.32E-08	1.66	17807
GO:0033993	response to lipid	2.31E-11	4.52E-08	2.97	17807
GO:0048583	regulation of response to stimulus	5.84E-11	1.02E-07	1.88	17807
GO:0002684	positive regulation of immune system process	6.11E-11	9.55E-08	3.33	17807
GO:0006952	defense response	6.33E-11	8.99E-08	3.33	17807
GO:0014070	response to organic cyclic compound	8.36E-11	1.09E-07	2.86	17807
GO:0048522	positive regulation of cellular process	1.37E-10	1.65E-07	1.68	17807
GO:0010033	response to organic substance	1.58E-10	1.77E-07	2.05	17807
GO:0042127	regulation of cell proliferation	1.64E-10	1.71E-07	2.49	17807
GO:0042221	response to chemical	2.00E-10	1.96E-07	1.93	17807
GO:0032496	response to lipopolysaccharide	5.99E-10	5.51E-07	4.4	17807
GO:0006950	response to stress	1.17E-09	1.01E-06	2	17807
GO:0002237	response to molecule of bacterial origin	1.31E-09	1.08E-06	4.24	17807
GO:0002682	regulation of immune system process	1.35E-09	1.06E-06	2.66	17807
GO:0071310	cellular response to organic substance	5.76E-09	4.29E-06	2.3	17807
GO:0001932	regulation of protein phosphorylation	5.82E-09	4.14E-06	2.47	17807
GO:0050727	regulation of inflammatory response	6.67E-09	4.53E-06	4.61	17807
GO:0042325	regulation of phosphorylation	8.37E-09	5.45E-06	2.38	17807
GO:0006954	inflammatory response	1.18E-08	7.40E-06	4.46	17807
GO:0042493	response to drug	1.45E-08	8.73E-06	2.61	17807
GO:0048584	positive regulation of response to stimulus	1.47E-08	8.50E-06	2.12	17807
GO:0009719	response to endogenous stimulus	1.55E-08	8.66E-06	2.39	17807
GO:0008284	positive regulation of cell proliferation	1.63E-08	8.81E-06	2.78	17807
GO:0051707	response to other organism	2.16E-08	1.13E-05	3.36	17807
GO:0009725	response to hormone	2.29E-08	1.16E-05	2.69	17807
GO:1901700	response to oxygen-containing compound	3.03E-08	1.48E-05	2.17	17807
GO:0051704	multi-organism process	3.08E-08	1.46E-05	2.71	17807
GO:0030155	regulation of cell adhesion	3.22E-08	1.48E-05	3.21	17807
GO:0050776	regulation of immune response	4.00E-08	1.79E-05	3.1	17807
GO:0048519	negative regulation of biological process	4.11E-08	1.78E-05	1.59	17807
GO:0019220	regulation of phosphate metabolic process	4.46E-08	1.88E-05	2.21	17807
GO:0051174	regulation of phosphorus metabolic process	4.55E-08	1.87E-05	2.21	17807
GO:0031349	positive regulation of defense response	5.33E-08	2.14E-05	4.5	17807
GO:0051239	regulation of multicellular organismal process	9.48E-08	3.71E-05	1.8	17807
GO:0070887	cellular response to chemical stimulus	1.05E-07	4.02E-05	2.05	17807
GO:0002376	immune system process	1.11E-07	4.12E-05	2.39	17807
GO:0007154	cell communication	1.29E-07	4.70E-05	3.08	17807
GO:0032879	regulation of localization	1.45E-07	5.17E-05	1.85	17807
GO:0048585	negative regulation of response to stimulus	1.82E-07	6.32E-05	2.23	17807
GO:0009617	response to bacterium	1.88E-07	6.40E-05	3.96	17807
GO:0051384	response to glucocorticoid	3.08E-07	1.03E-04	4.46	17807
GO:0050793	regulation of developmental process	3.28E-07	1.07E-04	1.86	17807
GO:1901654	response to ketone	3.74E-07	1.19E-04	3.97	17807
GO:0048545	response to steroid hormone	3.88E-07	1.21E-04	3.79	17807
GO:0032102	negative regulation of response to external stimulus	4.53E-07	1.39E-04	4.11	17807
GO:0051716	cellular response to stimulus	5.31E-07	1.60E-04	1.78	17807
GO:0051270	regulation of cellular component movement	5.59E-07	1.65E-04	2.53	17807
GO:0030334	regulation of cell migration	7.07E-07	2.05E-04	2.65	17807
GO:0031399	regulation of protein modification process	7.40E-07	2.11E-04	2.06	17807
GO:2000145	regulation of cell motility	7.46E-07	2.08E-04	2.6	17807
GO:0051240	ositive regulation of multicellular organismal proces	7.62E-07	2.09E-04	2.02	17807
GO:0031960	response to corticosteroid	9.40E-07	2.53E-04	4.12	17807
GO:0050878	regulation of body fluid levels	1.18E-06	3.13E-04	4.05	17807
GO:0040012	regulation of locomotion	1.47E-06	3.84E-04	2.47	17807
GO:0006955	immune response	1.80E-06	4.61E-04	2.91	17807
GO:0050729	positive regulation of inflammatory response	1.98E-06	5.01E-04	6.1	17807
GO:0009966	regulation of signal transduction	2.05E-06	5.09E-04	1.74	17807
GO:0034097	response to cytokine	2.20E-06	5.38E-04	2.74	17807
GO:0010941	regulation of cell death	2.39E-06	5.74E-04	2.04	17807
GO:1902531	regulation of intracellular signal transduction	2.55E-06	6.04E-04	2.03	17807
GO:0010942	positive regulation of cell death	2.61E-06	6.09E-04	2.78	17807
GO:0010647	positive regulation of cell communication	3.21E-06	7.38E-04	1.99	17807
GO:1901655	cellular response to ketone	3.51E-06	7.96E-04	5.22	17807
GO:0023051	regulation of signaling	3.54E-06	7.90E-04	1.65	17807
GO:0023056	positive regulation of signaling	3.64E-06	8.02E-04	1.98	17807
GO:0009628	response to abiotic stimulus	3.94E-06	8.56E-04	2.16	17807
GO:0031348	negative regulation of defense response	3.96E-06	8.47E-04	4.75	17807
GO:0032103	positive regulation of response to external stimulus	4.14E-06	8.74E-04	3.89	17807
GO:0040017	positive regulation of locomotion	4.36E-06	9.08E-04	2.93	17807
GO:0045088	regulation of innate immune response	4.41E-06	9.08E-04	4.1	17807
GO:0070663	regulation of leukocyte proliferation	4.46E-06	9.05E-04	4.37	17807
GO:0071549	cellular response to dexamethasone stimulus	4.65E-06	9.31E-04	8.43	17807
GO:0030595	leukocyte chemotaxis	4.98E-06	9.85E-04	6.21	17807
GO:0050865	regulation of cell activation	5.43E-06	1.06E-03	2.98	17807
GO:0006935	chemotaxis	5.53E-06	1.07E-03	4.02	17807
GO:0002694	regulation of leukocyte activation	5.58E-06	1.07E-03	3.07	17807
GO:0010646	regulation of cell communication	5.79E-06	1.09E-03	1.64	17807
GO:0070372	regulation of ERK1 and ERK2 cascade	6.54E-06	1.22E-03	3.75	17807
GO:0042330	taxis	6.60E-06	1.21E-03	3.96	17807
GO:0031668	cellular response to extracellular stimulus	7.85E-06	1.43E-03	3.91	17807
GO:0048523	negative regulation of cellular process	7.86E-06	1.41E-03	1.51	17807
GO:0007166	cell surface receptor signaling pathway	8.09E-06	1.44E-03	2.03	17807
GO:0065008	regulation of biological quality	8.40E-06	1.48E-03	1.59	17807
GO:0009611	response to wounding	9.31E-06	1.62E-03	3.85	17807
GO:0051272	positive regulation of cellular component movement	9.39E-06	1.61E-03	2.88	17807
GO:0042327	positive regulation of phosphorylation	1.02E-05	1.73E-03	2.29	17807
GO:0001934	positive regulation of protein phosphorylation	1.04E-05	1.76E-03	2.33	17807
GO:0051128	regulation of cellular component organization	1.06E-05	1.76E-03	1.75	17807
GO:0071407	cellular response to organic cyclic compound	1.08E-05	1.78E-03	2.94	17807
GO:0030335	positive regulation of cell migration	1.08E-05	1.76E-03	2.94	17807
GO:0042060	wound healing	1.11E-05	1.79E-03	5.68	17807
GO:0000278	mitotic cell cycle	1.36E-05	2.17E-03	5.55	17807
GO:0032268	regulation of cellular protein metabolic process	1.50E-05	2.37E-03	1.73	17807

GO:0002683	negative regulation of immune system process	1.55E-05	2.42E-03	3.08	17807
GO:0098542	defense response to other organism	1.71E-05	2.65E-03	3.31	17807
GO:0002697	regulation of immune effector process	1.77E-05	2.72E-03	3.3	17807
GO:2000147	positive regulation of cell motility	1.90E-05	2.89E-03	2.83	17807
GO:0071496	cellular response to external stimulus	2.10E-05	3.16E-03	3.26	17807
GO:0016043	cellular component organization	2.21E-05	3.30E-03	1.48	17807
GO:0051241	egative regulation of multicellular organismal proces	2.33E-05	3.44E-03	2.08	17807
GO:0040011	locomotion	2.40E-05	3.50E-03	2.31	17807
GO:0090025	regulation of monocyte chemotaxis	2.46E-05	3.56E-03	13.98	17807
GO:0009991	response to extracellular stimulus	2.53E-05	3.64E-03	2.56	17807
GO:0045595	regulation of cell differentiation	2.58E-05	3.67E-03	1.86	17807
GO:0032502	developmental process	2.71E-05	3.82E-03	1.45	17807
GO:0051246	regulation of protein metabolic process	2.74E-05	3.83E-03	1.68	17807
GO:0034405	response to fluid shear stress	2.91E-05	4.02E-03	9.91	17807
GO:0044319	wound healing, spreading of cells	2.98E-05	4.09E-03	13.46	17807
GO:0032355	response to estradiol	3.08E-05	4.18E-03	3.92	17807
GO:0071495	cellular response to endogenous stimulus	3.23E-05	4.35E-03	2.27	17807
GO:1902532	egative regulation of intracellular signal transductior	3.25E-05	4.34E-03	2.82	17807
GO:2000026	regulation of multicellular organismal development	3.29E-05	4.36E-03	1.78	17807
GO:0071396	cellular response to lipid	3.33E-05	4.38E-03	2.73	17807
GO:0071840	cellular component organization or biogenesis	3.43E-05	4.46E-03	1.46	17807
GO:0043408	regulation of MAPK cascade	3.43E-05	4.43E-03	2.45	17807
GO:0007049	cell cycle	3.50E-05	4.49E-03	4.52	17807
GO:0010562	positive regulation of phosphorus metabolic process	3.87E-05	4.92E-03	2.14	17807
GO:0045937	positive regulation of phosphate metabolic process	3.87E-05	4.88E-03	2.14	17807
GO:1902533	ositive regulation of intracellular signal transduction	4.06E-05	5.08E-03	2.2	17807
GO:0007059	chromosome segregation	4.26E-05	5.29E-03	6.25	17807
GO:0048870	cell motility	4.39E-05	5.40E-03	2.32	17807
GO:0016477	cell migration	4.65E-05	5.68E-03	2.41	17807
GO:0007159	leukocyte cell-cell adhesion	4.83E-05	5.85E-03	9.09	17807
GO:0045087	innate immune response	5.08E-05	6.12E-03	3.73	17807
GO:0045597	positive regulation of cell differentiation	5.34E-05	6.38E-03	2.14	17807
GO:0071548	response to dexamethasone	5.36E-05	6.34E-03	6.06	17807
GO:0051249	regulation of lymphocyte activation	5.64E-05	6.63E-03	3.01	17807
GO:0050670	regulation of lymphocyte proliferation	5.83E-05	6.81E-03	3.95	17807
GO:0030193	regulation of blood coagulation	5.90E-05	6.83E-03	7.07	17807
GO:0050730	regulation of peptidyl-tyrosine phosphorylation	5.97E-05	6.86E-03	3.68	17807
GO:0060326	cell chemotaxis	6.07E-05	6.93E-03	4.25	17807
GO:0001525	angiogenesis	6.36E-05	7.21E-03	3.91	17807
GO:0032944	regulation of mononuclear cell proliferation	6.36E-05	7.16E-03	3.91	17807
GO:1900046	regulation of hemostasis	6.45E-05	7.20E-03	6.97	17807
GO:0009266	response to temperature stimulus	6.64E-05	7.36E-03	3.89	17807
GO:0071466	cellular response to xenobiotic stimulus	6.67E-05	7.35E-03	5.87	17807
GO:0042542	response to hydrogen peroxide	6.82E-05	7.46E-03	4.6	17807
GO:0006928	movement of cell or subcellular component	6.92E-05	7.51E-03	2.05	17807
GO:0043067	regulation of programmed cell death	7.27E-05	7.84E-03	1.9	17807
GO:0002699	positive regulation of immune effector process	7.54E-05	8.08E-03	3.84	17807
GO:0001817	regulation of cytokine production	7.69E-05	8.18E-03	2.5	17807
GO:0061041	regulation of wound healing	7.91E-05	8.36E-03	5.03	17807
GO:0050818	regulation of coagulation	8.35E-05	8.77E-03	6.69	17807
GO:0016264	gap junction assembly	8.64E-05	9.01E-03	31.15	17807
GO:0002685	regulation of leukocyte migration	8.83E-05	9.14E-03	4.08	17807
GO:1901698	response to nitrogen compound	9.26E-05	9.52E-03	2.02	17807
GO:0008360	regulation of cell shape	9.44E-05	9.65E-03	4.92	17807
GO:0071345	cellular response to cytokine stimulus	9.80E-05	9.95E-03	2.6	17807
GO:0048869	cellular developmental process	1.00E-04	1.01E-02	1.6	17807
GO:0071385	cellular response to glucocorticoid stimulus	1.01E-04	1.02E-02	5.54	17807
GO:0002675	positive regulation of acute inflammatory response	1.10E-04	1.09E-02	10.38	17807
GO:0051094	positive regulation of developmental process	1.10E-04	1.09E-02	1.88	17807
GO:1903034	regulation of response to wounding	1.14E-04	1.12E-02	4.33	17807
GO:0010810	regulation of cell-substrate adhesion	1.15E-04	1.13E-02	3.96	17807
GO:0042981	regulation of apoptotic process	1.16E-04	1.13E-02	1.88	17807
GO:0050867	positive regulation of cell activation	1.25E-04	1.20E-02	3.23	17807
GO:0009408	response to heat	1.25E-04	1.20E-02	4.74	17807
GO:0043434	response to peptide hormone	1.26E-04	1.20E-02	2.82	17807
GO:0010038	response to metal ion	1.26E-04	1.19E-02	2.72	17807
GO:0031099	regeneration	1.28E-04	1.20E-02	3.63	17807
GO:0010035	response to inorganic substance	1.28E-04	1.20E-02	2.36	17807
GO:0007346	regulation of mitotic cell cycle	1.29E-04	1.20E-02	2.71	17807
GO:0009967	positive regulation of signal transduction	1.30E-04	1.20E-02	1.87	17807
GO:1901987	regulation of cell cycle phase transition	1.32E-04	1.21E-02	3.4	17807
GO:1905954	positive regulation of lipid localization	1.35E-04	1.24E-02	6.2	17807
GO:0001933	negative regulation of protein phosphorylation	1.41E-04	1.28E-02	2.91	17807
GO:0045785	positive regulation of cell adhesion	1.41E-04	1.28E-02	2.91	17807
GO:1901701	cellular response to oxygen-containing compound	1.43E-04	1.29E-02	2.06	17807
GO:0046640	regulation of alpha-beta T cell proliferation	1.44E-04	1.29E-02	9.82	17807
GO:0034103	regulation of tissue remodeling	1.46E-04	1.30E-02	6.13	17807
GO:0071384	cellular response to corticosteroid stimulus	1.49E-04	1.32E-02	5.24	17807
GO:0022603	regulation of anatomical structure morphogenesis	1.67E-04	1.47E-02	2.07	17807
GO:0031669	cellular response to nutrient levels	1.67E-04	1.46E-02	3.53	17807
GO:0022414	reproductive process	1.73E-04	1.50E-02	1.86	17807
GO:1901990	regulation of mitotic cell cycle phase transition	1.74E-04	1.50E-02	3.52	17807
GO:0010243	response to organonitrogen compound	1.75E-04	1.50E-02	2	17807
GO:0050900	leukocyte migration	1.83E-04	1.56E-02	4.08	17807
GO:0010652	ve regulation of cell communication by chemical cou	1.89E-04	1.60E-02	72.68	17807
GO:0010645	gulation of cell communication by chemical couplin	1.89E-04	1.59E-02	72.68	17807
GO:0003294	atrial ventricular junction remodeling	1.89E-04	1.59E-02	72.68	17807
GO:0070667	negative regulation of mast cell proliferation	1.89E-04	1.58E-02	72.68	17807
GO:0007155	cell adhesion	1.91E-04	1.59E-02	2.41	17807
GO:0006979	response to oxidative stress	1.92E-04	1.59E-02	2.83	17807
GO:0070664	negative regulation of leukocyte proliferation	1.96E-04	1.62E-02	5.85	17807
GO:0010604	sitive regulation of macromolecule metabolic proces	1.98E-04	1.62E-02	1.53	17807
GO:0071498	cellular response to fluid shear stress	2.10E-04	1.71E-02	13.21	17807
GO:1903532	positive regulation of secretion by cell	2.19E-04	1.78E-02	2.69	17807
GO:0051591	response to cAMP	2.24E-04	1.80E-02	4.39	17807
GO:0034754	cellular hormone metabolic process	2.26E-04	1.81E-02	5.72	17807
GO:0022610	biological adhesion	2.26E-04	1.81E-02	2.38	17807
GO:0050778	positive regulation of immune response	2.30E-04	1.82E-02	2.59	17807
GO:0009888	tissue development	2.31E-04	1.83E-02	2.37	17807
GO:0000226	microtubule cytoskeleton organization	2.43E-04	1.91E-02	3.03	17807

GO:0051172	ative regulation of nitrogen compound metabolic pro	2.46E-04	1.92E-02	1.64	17807
GO:0051896	regulation of protein kinase B signaling	2.47E-04	1.92E-02	4.33	17807
GO:0050777	negative regulation of immune response	2.47E-04	1.91E-02	4.33	17807
GO:0065009	regulation of molecular function	2.48E-04	1.91E-02	1.54	17807
GO:0050896	response to stimulus	2.62E-04	2.01E-02	1.31	17807
GO:0014074	response to purine-containing compound	2.63E-04	2.01E-02	3.6	17807
GO:0010605	gative regulation of macromolecule metabolic proce	2.64E-04	2.01E-02	1.61	17807
GO:0051047	positive regulation of secretion	2.65E-04	2.00E-02	2.56	17807
GO:0002696	positive regulation of leukocyte activation	2.77E-04	2.09E-02	3.15	17807
GO:0032870	cellular response to hormone stimulus	2.82E-04	2.11E-02	2.63	17807
GO:0070486	leukocyte aggregation	2.87E-04	2.14E-02	21.8	17807
GO:0002673	regulation of acute inflammatory response	2.91E-04	2.16E-02	6.61	17807
GO:0046635	positive regulation of alpha-beta T cell activation	2.91E-04	2.15E-02	6.61	17807
GO:0032269	gative regulation of cellular protein metabolic proce	2.93E-04	2.15E-02	2.03	17807
GO:0046641	positive regulation of alpha-beta T cell proliferation	2.99E-04	2.19E-02	12.11	17807
GO:0031667	response to nutrient levels	3.02E-04	2.20E-02	2.33	17807
GO:0030154	cell differentiation	3.03E-04	2.19E-02	1.71	17807
GO:0010564	regulation of cell cycle process	3.14E-04	2.26E-02	2.45	17807
GO:0042509	gulation of tyrosine phosphorylation of STAT protein	3.16E-04	2.27E-02	6.51	17807
GO:0050731	ositive regulation of peptidyl-tyrosine phosphorylatio	3.23E-04	2.30E-02	3.81	17807
GO:0046683	response to organophosphorus	3.23E-04	2.29E-02	3.81	17807
GO:0031401	positive regulation of protein modification process	3.31E-04	2.34E-02	1.93	17807
GO:0051248	negative regulation of protein metabolic process	3.33E-04	2.34E-02	1.98	17807
GO:1901652	response to peptide	3.34E-04	2.34E-02	2.51	17807
GO:0043065	positive regulation of apoptotic process	3.45E-04	2.41E-02	2.36	17807
GO:0033043	regulation of organelle organization	3.46E-04	2.40E-02	1.93	17807
GO:1903530	regulation of secretion by cell	3.51E-04	2.43E-02	2.15	17807
GO:0071383	cellular response to steroid hormone stimulus	3.56E-04	2.46E-02	4.61	17807
GO:0009636	response to toxic substance	3.74E-04	2.56E-02	2.41	17807
GO:1902107	positive regulation of leukocyte differentiation	3.79E-04	2.59E-02	4.09	17807
GO:0042326	negative regulation of phosphorylation	3.81E-04	2.59E-02	2.66	17807
GO:0043068	positive regulation of programmed cell death	3.82E-04	2.59E-02	2.34	17807
GO:0009893	positive regulation of metabolic process	3.84E-04	2.59E-02	1.47	17807
GO:0033273	response to vitamin	3.97E-04	2.66E-02	4.06	17807
GO:0032570	response to progesterone	4.01E-04	2.68E-02	6.23	17807
GO:0050789	regulation of biological process	4.03E-04	2.68E-02	1.17	17807
GO:0043069	negative regulation of programmed cell death	4.10E-04	2.72E-02	2.05	17807
GO:1903708	positive regulation of hemopoiesis	4.29E-04	2.83E-02	3.67	17807
GO:0033280	response to vitamin D	4.53E-04	2.98E-02	7.73	17807
GO:1903047	mitotic cell cycle process	4.63E-04	3.03E-02	2.72	17807
GO:0033138	ositive regulation of peptidyl-serine phosphorylation	4.63E-04	3.02E-02	5.09	17807
GO:0046634	regulation of alpha-beta T cell activation	4.63E-04	3.00E-02	5.09	17807
GO:0046677	response to antibiotic	4.66E-04	3.01E-02	2.52	17807
GO:0009892	negative regulation of metabolic process	4.73E-04	3.04E-02	1.55	17807
GO:1902105	regulation of leukocyte differentiation	4.91E-04	3.14E-02	3.14	17807
GO:0042129	regulation of T cell proliferation	4.96E-04	3.17E-02	3.94	17807
GO:0097327	response to antineoplastic agent	4.96E-04	3.15E-02	3.94	17807
GO:0071675	regulation of mononuclear cell migration	5.00E-04	3.17E-02	7.57	17807
GO:0070373	negative regulation of ERK1 and ERK2 cascade	5.03E-04	3.17E-02	5.97	17807
GO:0033135	regulation of peptidyl-serine phosphorylation	5.12E-04	3.22E-02	4.37	17807
GO:0071377	cellular response to glucagon stimulus	5.16E-04	3.23E-02	18.17	17807
GO:0060255	regulation of macromolecule metabolic process	5.22E-04	3.25E-02	1.34	17807
GO:0000302	response to reactive oxygen species	5.28E-04	3.28E-02	3.32	17807
GO:0071363	cellular response to growth factor stimulus	5.28E-04	3.26E-02	2.8	17807
GO:0007088	regulation of mitotic nuclear division	5.41E-04	3.33E-02	3.89	17807
GO:0051046	regulation of secretion	5.52E-04	3.39E-02	2.05	17807
GO:0002072	p morphogenesis involved in camera-type eye devel	5.60E-04	3.42E-02	48.45	17807
GO:0010643	cell communication by chemical coupling	5.60E-04	3.41E-02	48.45	17807
GO:1990408	citonin gene-related peptide receptor signaling pathv	5.60E-04	3.40E-02	48.45	17807
GO:0051754	meiotic sister chromatid cohesion, centromeric	5.60E-04	3.38E-02	48.45	17807
GO:0070848	response to growth factor	5.82E-04	3.50E-02	2.66	17807
GO:0071347	cellular response to interleukin-1	5.86E-04	3.51E-02	4.89	17807
GO:0051247	positive regulation of protein metabolic process	5.88E-04	3.51E-02	1.73	17807
GO:0009612	response to mechanical stimulus	5.93E-04	3.53E-02	3.07	17807
GO:0050728	negative regulation of inflammatory response	5.94E-04	3.52E-02	4.28	17807
GO:0032970	regulation of actin filament-based process	6.04E-04	3.56E-02	2.77	17807
GO:0035313	wound healing, spreading of epidermal cells	6.64E-04	3.91E-02	16.77	17807
GO:0032270	ositive regulation of cellular protein metabolic proces	7.02E-04	4.11E-02	1.75	17807
GO:0043066	negative regulation of apoptotic process	7.03E-04	4.10E-02	2.01	17807
GO:0050863	regulation of T cell activation	7.12E-04	4.14E-02	3.01	17807
GO:0042572	retinol metabolic process	7.23E-04	4.19E-02	9.69	17807
GO:1903706	regulation of hemopoiesis	7.26E-04	4.19E-02	2.71	17807
GO:0031324	negative regulation of cellular metabolic process	7.31E-04	4.20E-02	1.56	17807
GO:0007017	microtubule-based process	7.32E-04	4.19E-02	2.35	17807
GO:0032526	response to retinoic acid	7.53E-04	4.30E-02	4.12	17807
GO:0051251	positive regulation of lymphocyte activation	7.64E-04	4.34E-02	3.17	17807
GO:0001649	osteoblast differentiation	7.67E-04	4.35E-02	5.52	17807
GO:0070555	response to interleukin-1	7.89E-04	4.45E-02	4.09	17807
GO:0045824	negative regulation of innate immune response	7.93E-04	4.46E-02	6.86	17807
GO:0043900	regulation of multi-organism process	8.05E-04	4.51E-02	2.68	17807
GO:0006898	receptor-mediated endocytosis	8.19E-04	4.58E-02	3.67	17807
GO:0030261	chromosome condensation	8.22E-04	4.57E-02	9.38	17807
GO:0008285	negative regulation of cell proliferation	8.50E-04	4.71E-02	2.2	17807
GO:0034612	response to tumor necrosis factor	8.53E-04	4.71E-02	3.65	17807
GO:0048661	ositive regulation of smooth muscle cell proliferation	8.64E-04	4.76E-02	4.58	17807
GO:1903035	negative regulation of response to wounding	8.75E-04	4.80E-02	5.38	17807
GO:0070665	positive regulation of leukocyte proliferation	9.04E-04	4.95E-02	4.01	17807
GO:0007568	aging	9.23E-04	5.03E-02	2.54	17807
GO:0031670	cellular response to nutrient	9.34E-04	5.07E-02	5.32	17807
GO:0016101	diterpenoid metabolic process	9.40E-04	5.09E-02	6.61	17807
GO:0090066	regulation of anatomical structure size	9.45E-04	5.09E-02	2.54	17807
GO:0065007	biological regulation	9.55E-04	5.13E-02	1.15	17807
GO:0002703	regulation of leukocyte mediated immunity	9.69E-04	5.19E-02	3.3	17807
GO:0071222	cellular response to lipopolysaccharide	9.69E-04	5.17E-02	3.3	17807
GO:0019222	regulation of metabolic process	9.75E-04	5.19E-02	1.3	17807
GO:0060548	negative regulation of cell death	9.80E-04	5.20E-02	1.91	17807

Supplementary Table 2. 295 genes were significantly up- or downregulated after sTNFR1 injection. Terms from Gene Ontology analysis indicate that 95 of 295 (32.2%) differentially expressed genes were related to inflammatory processes. Columns 1 and 2 indicate the specific Gene Ontology term numbers and descriptions. P-value indicates nominal significance value for each gene, while FDR q-value reflects the adjusted value accounting for false discovery rate. Enrichment score indicates the degree to which the genes are overrepresented at the top or bottom of the entire ranked list of genes.